Lasers in Surgery and Medicine 24:38–47 (1999)

Measurement of Thermal Effects on the Optical Properties of Prostate Tissue at Wavelengths of 1,064 and 633 nm

William H. Nau, PhD,[1]* Robert J. Roselli, PhD,[1] and Douglas F. Milam, MD[2]

[1]Department of Biomedical Engineering, Vanderbilt University, Nashville, Tennessee 37235
[2]Department of Urology, Vanderbilt University Medical Center, Nashville, Tennessee 37235

Background and Objective: **The extent of thermal injury during laser prostatectomy is dependent on the light distribution in laser-irradiated tissue. As tissue is irradiated, the optical properties change as a function of temperature due to an alteration of molecular and cellular structure. The purpose of the present study was to determine how the exposure of both fresh and previously frozen canine prostate tissue to elevated temperatures affects the optical properties.**
Study Design/Materials and Methods: **Optical properties were measured by using a double integrating sphere spectrophotometer with an inverse adding-doubling algorithm. Measurements were made at two wavelengths (1,064 nm and 633 nm) on samples heated in a waterbath in 5°–10° increments for 10 min through a 50°C temperature range.**
Results: **Upon coagulation, the absorption coefficient of fresh tissue decreased from the baseline measurement for both wavelengths (0.027 ± 0.003 to 0.019 ± 0.002 for λ = 1,064 nm; 0.073 ± 0.007 to 0.061 ± 0.006 for λ = 633 nm). However, the scattering coefficient increased sharply from the baseline measurement following coagulation (3.06 ± 0.26 to 6.05 ± 0.29 for λ = 1,064 nm; 4.89 ± 0.23 to 7.22 ± 0.30 for λ = 633 nm). Thermal coagulation occurred during exposure to temperatures between 60°C and 70°C.**
Conclusion: **Data obtained in this study indicate that thermal coagulation of tissue alters the optical properties. The extent to which these changes occur was found to be dependent on wavelength and freshness of tissue. These results are significant because they suggest how thermally induced changes in the optical properties may limit the depth of light penetration in tissue thus compromising treatment. Lasers Surg. Med. 24:38–47, 1999.**

Key words: integrating spheres; absorption coefficient; scattering coefficient; anisotropy coefficient; benign prostatic hyperplasia; cryopreservation

INTRODUCTION

Absorption and scattering of laser light are important in predicting the extent of tissue injury during laser prostatectomy. As tissue is irradiated, light traveling through the tissue is attenuated by absorption and scattering. The propor-

Contract grant sponsor: Department of Urology, Vanderbilt University Medical Center, Nashville, Tennessee.

*Correspondence to: William H. Nau, PhD, Department of Radiation Oncology, University of California, San Francisco, 505 Parnassus Avenue, Box 0226 Room L-75, San Francisco, CA 94143-0226. E-mail: nau@itsa.ucsf.edu

Accepted 25 August 1998

tionality constant describing the amount of light attenuated by absorption is called the absorption coefficient (μ_a). The constant describing the attenuation of light due to scattering away from the direction of propagation is the scattering coefficient (μ_s). The anisotropy coefficient (g) is a parameter that describes the fraction of light scattered into any given direction and is equal to the average cosine of the scattering angle [1]. Another parameter, known as the reduced scattering coefficient [$\mu_s' = \mu_s \cdot (1 - g)$], is also used to describe scattering in anisotropic materials. These coefficients are referred to as the optical properties. An understanding of these properties is important for the rational design of interstitial, refractive, and reflective laser therapy devices. Because the distribution of light in tissue is dependent on tissue optics, much research on measuring the optical properties of tissues has been conducted, and several methods have been introduced [2–7].

Optical properties of tissue have been shown to be temperature dependent. This is of concern because an increase in the absorption or scattering coefficient prevents light from penetrating deeper into the tissue, thus compromising laser treatment. Temperature-dependent changes in total reflectance and transmittance have been measured while irradiating excised atrial wall specimens [8]. It was found that with the higher irradiance, transmittance decreases rapidly with increasing temperature to the point of coagulation, which is followed by a rapid increase in transmittance as temperatures continue to increase. Reflectance measurements showed inverse responses. Another study has reported a fourfold increase in the scattering coefficient (0.43–1.74 mm^{-1}) of porcine myocardium during coagulation, whereas the absorption coefficient remained relatively unchanged (0.04 to 0.05 mm^{-1}) [9]. Similar results have been demonstrated in canine and human coagulated myocardial tissue [5]. In rat liver, the scattering coefficient has been shown to increase while the absorption and anisotropy coefficients decrease during tissue heating [10].

Tissue samples are often frozen after excision to prevent autolysis until they can be measured or to aid in obtaining thin slices. A study of the effects of cryopreservation on the optical properties of human aorta have demonstrated a decrease in the absorption coefficient by as much as 11% and an increase of up to 43% in the reduced scattering coefficient as compared with fresh tissue [11].

Whether data obtained from animal models can be extrapolated to the human patient remains a concern. No significant difference has been found between the optical properties of human and canine myocardium at 1,064 nm [5], but canine bladder tissue has been found to have a 70% higher scattering coefficient (5.08 mm^{-1}) than human bladder (2.93 mm^{-1}) at a wavelength of 633 nm [12]. It is apparent from these results that differences in the optical properties between human and animal tissue are organ dependent.

A double-integrating-sphere system has been used to determine absorption and scattering coefficients of tissue [13]. Measurements of the total reflectance and transmittance are used in conjunction with an inverse-adding-doubling (IAD) algorithm to calculate the optical coefficients [14]. This system has been used to measure optical properties of healthy and diseased breast tissue [15].

The purpose of the present study was to determine whether exposure of canine prostate tissue to increasing temperatures affects the optical properties of the tissue. The effects of freezing tissue prior to measurement of optical properties and differences in these properties between human and canine prostate were also investigated. In addition, the sensitivity of the IAD method to the effect of measurement errors was investigated.

MATERIALS AND METHODS

Experimental Setup

All measurements were obtained by using a double-integrating sphere system (see Fig. 1). This apparatus consisted of two integrating spheres (model 70451, Oriel Corporation, Stratford, CT), and a collimated laser source focused to a 2-mm spot size. Two wavelengths were chosen for this study: an Nd:YAG surgical laser (λ = 1,064 nm, with a 600-μ end-firing fiber, Surgical Laser Technologies, Inc., Montgomeryville, PA), and its HeNe aiming beam (λ = 633 nm). Photodiodes (model S2386-18K, Hamamatsu Corporation) (Hamamatsu Photonics, Bridgewater, NJ) embedded within the sphere walls were used to measure the diffuse reflected and diffuse transmitted light. A third detector was aligned behind a pin hole 60 cm from the transmittance sphere to detect unscattered collimated light. Light measured by the detectors was converted to a voltage, amplified by a three-channel, three-stage ampli-

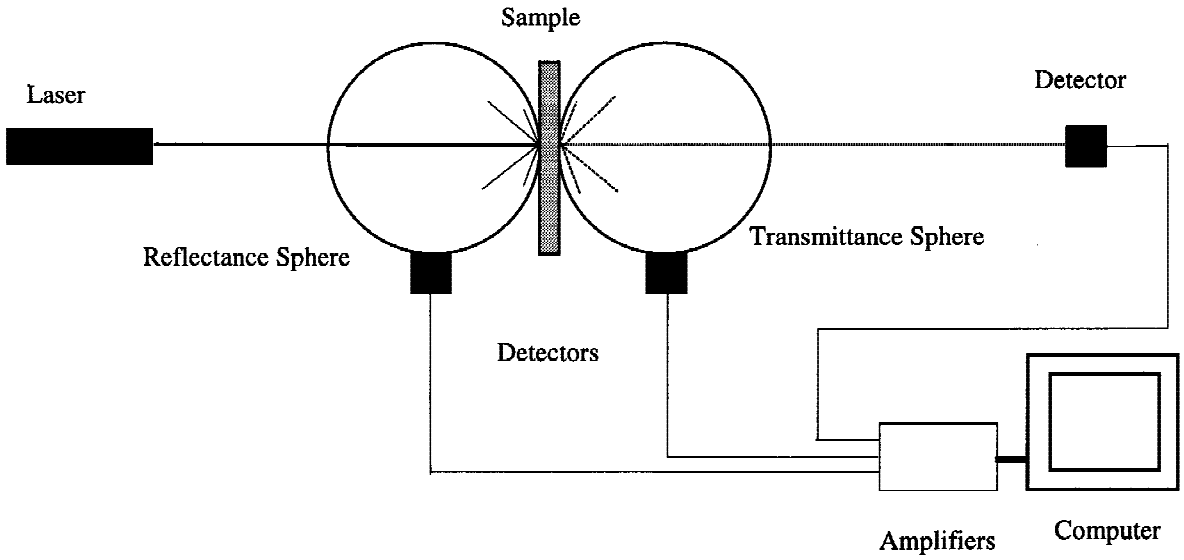

Fig. 1. Double-integrating sphere setup.

fier, and collected and displayed on a computer with a data acquisition card (DAS-8, Metrabyte, Cleveland, OH).

Sample Preparation

Prostates were surgically removed from dogs killed by exsanguination and were cut into approximately 1–2-mm-thick slices. Each slice was placed between two 76 × 50 × 1.2-mm glass microscope slides. A drop of water was placed between the tissue sample and the glass slides to reduce mismatches in the optical boundaries. The slides were then sealed at the edges with rolled paraffin film to prevent dehydration during the measurements. The total thickness of each sample was measured with a pair of calipers, and the thickness of glass slides was subtracted from the total to determine sample thickness.

Measurement Procedure

Reference measurements were made for each sphere with a 99% reflectance standard, and the amplifier gain was adjusted until the maximum output was 9 V. The samples were sealed in a plastic bag, and placed in a waterbath at 35°C for 10 min to allow them to reach constant temperature. Previous thermal measurements on samples of different thicknesses with thermistor probes embedded in them assured that this time frame was sufficient to allow the samples to reach thermal equilibrium with the waterbath.

The samples were then removed from the waterbath, placed between the integrating spheres, and irradiated in continuous wave mode while recording the reflectance and transmittance voltages (approximately 5 sec). For the Nd:YAG laser, a beam intensity of 50 mW was used to prevent the beam from inducing thermal changes in the tissue during the measurement process. The HeNe laser had a beam intensity of 0.5 mW. After recording the voltages, the samples were placed back into the waterbath for 10 min, with the temperature increased by 10°C. This procedure was repeated with 10°C temperature increments to 55°C and then in 5°C increments from 60°C to 85°C.

Implementation of the IAD Program

The IAD algorithm was [13,14,16] ported to a PC platform and implemented on a 66-MHz Pentium computer (model P5-66, Gateway 2000, North Sioux City, SD).

This algorithm requires at least two voltage measurements as input: the voltage measured in the reflectance sphere (V_r), and that measured in the transmittance sphere (V_t). The voltage measured by the collimated detector (V_c) may also be input, but it is not required by the program if g is known. These voltages must first be normalized to a reference measurement as

$$V\% = \frac{V - V_0}{V_{ref} - V_0} \quad (1)$$

where V% is the normalized voltage, V is the measurement with the sample in place, V_0 is the mea-

surement with no sample, and V_{ref} is the measurement with a 99% reflectance standard.

The IAD algorithm also requires values for the index of refraction (n) of the tissue and glass slides and for a default value for the anisotropy coefficient in the event that V_c% is zero. For this study, n of tissue was assumed to be 1.4. At each degree of coagulation, the calculated values of g from samples in which all three measured voltages were nonzero were averaged. For samples in which V_c% was immeasurable at a particular temperature, the averaged g values for that temperature point were used as the default g values in the algorithm. The resulting values from the algorithm for the albedo and optical thickness were used along with the sample thickness to calculate the absorption, scattering, and reduced scattering coefficients.

Effect of Frozen Storage

To determine whether freezing the tissue affected optical properties in the prostate, approximately 10 samples of frozen and then thawed canine prostate tissue were measured at each of the two wavelengths. Each sample had been stored at –70°C for at least 3 weeks and allowed to thaw to room temperature before making measurements.

Measurements on Human Tissue

To determine whether the optical properties of canine prostate tissue are similar to those of the human prostate, two anecdotal measurements were made on freshly excised samples of human prostate with the Nd:YAG laser source.

Evaluation of Sensitivity of IAD Algorithm

The sensitivity of the IAD algorithm to the four measured variables, the choice of anisotropy coefficient, and the value of the tissue index of refraction was investigated. Measurements from one fresh prostate sample irradiated with the 1,064-nm laser gave 0.44 for V_r%, 0.40 for V_t%, and 0.01 for V_c%. The values for the input parameters (n, d, V_r%, V_c%, and V_t%) were independently changed by ±1%, ±5%, ±10%, and ±20%. The percent difference between the newly calculated values of μ_a, μ_s, and g were then compared with the baseline values. To investigate how sensitive the computation of μ_a and μ_s were to an assumed value for g, V_c% was set to zero, and the value for g was changed between 0.4 and 0.8. The percent difference between the newly calculated values were compared with the baseline measurements.

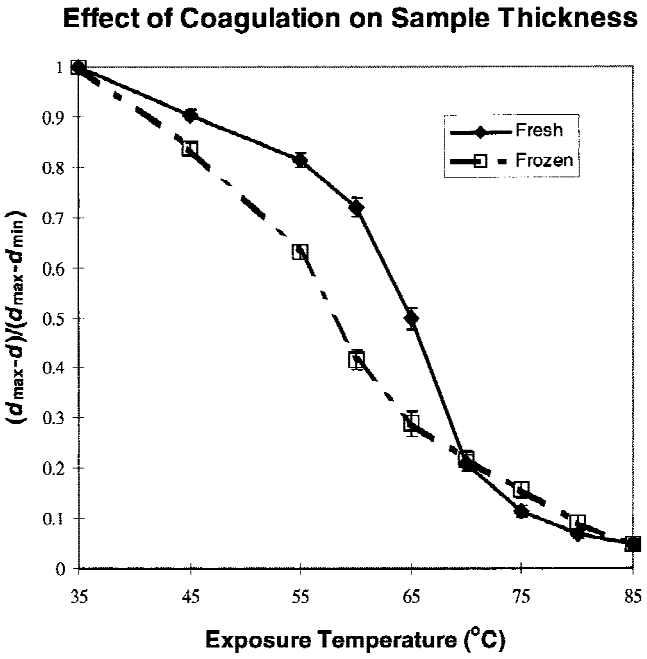

Fig. 2. Normalized change in sample thickness of fresh and previously frozen tissue samples during coagulation due to exposure to elevated temperatures (data points represent the mean ± SEM).

RESULTS

During the experiments, the samples changed in appearance and size as the tissue coagulated. The tissue started as slightly pink in color and then whitened as temperatures approached 65°C. The tissue then began to turn brownish gray in color as the exposure temperature was increased above 70°C. For temperatures above 80°C, the previously frozen samples began to disintegrate. Samples obtained from fresh tissue maintained their integrity throughout the experiment. The mean value of the initial sample thickness was measured at 1.09 ± 0.27 mm. A plot of the change in normalized sample thickness during heating is shown in Figure 2.

A summary of the optical properties determined in this study is presented in Table 1. A repeated measures analysis of variance (ANOVA) [17] was performed on the absorption and scattering coefficients by using the measurements at exposure temperatures of 35°C (baseline), 55°C, 60°C, and 70°C (complete coagulation).

In general, the absorption coefficient was seen to decrease with coagulation up to an exposure temperature of 65°C, followed by an increase (see Fig. 3). The increase in μ_a corresponded to a slight darkening of the tissue samples. The frozen

TABLE 1. Summary of Measured Optical Properties Before and After Coagulation (Values Reported as Mean ± SEM in mm^{-1})

λ (nm)	Tissue, n[a]	Baseline μ_a	Baseline μ_s	Baseline g[b]	Baseline μ_s'	Coagulated μ_a	Coagulated μ_s	Coagulated g[b]	Coagulated μ_s'
	Fresh, 7	0.027	3.06	0.45	1.76	0.019	6.05	0.59	2.44
		±0.003	±0.26	±0.03	±0.13	±0.002	±0.29	±0.04	±0.14
1064	Frozen, 10	0.071	4.22	0.81	0.79	0.047	10.62	0.77	2.94
		±0.006	±0.30	±0.01	±0.05	±0.006	±1.1	±0.01	±0.26
	Human, 2	0.078	1.66	0.63	0.63	0.075	2.13	0.51	1.08
		±0.003	±0.07	±0.05	±0.14	±0.002	±0.01	±0.07	±0.14
633	Fresh, 10	0.073	4.89	0.54	2.25	0.061	7.22	0.51	3.59
		±0.007	±0.23	±0.03	±0.05	±0.006	±0.30	±0.03	±0.17
	Frozen, 13	0.076	5.01	0.80	1.00	0.080	8.25	0.47	4.50
		±0.003	±0.57	±0.01	±0.11	±0.006	±0.48	±0.02	±0.26

[a]n is the number of samples in each group.
[b]g, average value from three samples.

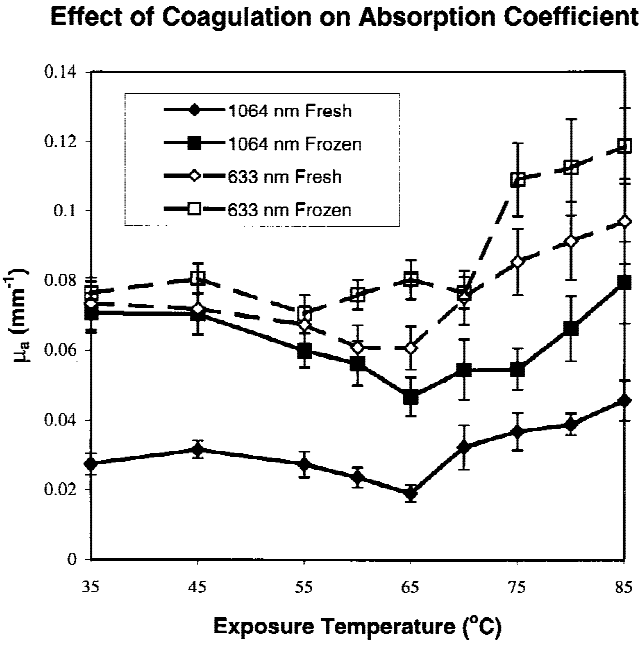

Fig. 3. Absorption coefficients for fresh and previously frozen canine prostate tissue measured at wavelengths of 1,064 and 633 nm (data points represent the mean ± SEM).

samples measured at 633 nm, however, did not exhibit the decrease in μ_a but remained constant (0.076 ± 0.003 mm^{-1}) up to 70°C before beginning to increase. The exposure temperature dependence for μ_a was confirmed by the ANOVA ($P < 0.05$). Values measured in frozen tissue were typically greater than those from the fresh samples in the 1,064-nm wavelength measurements (also confirmed by ANOVA, $P < 0.05$). A wavelength dependence was also noted ($P < 0.05$), but only the fresh sample values measured at 1,064 nm appeared to be considerably different than those measured at 633 nm (0.027 ± 0.003 vs. 0.073 ± 0.007 mm^{-1}).

As seen in Figure 4, the scattering coefficients measured at 1,064 nm exhibited a slight increase with exposure temperatures up 60°C (3.06 ± 0.26 to 3.88 ± 0.15 mm^{-1} for fresh, 4.22 ± 0.30 to 6.78 ± 0.48 for frozen). Between the temperatures of 60°C and 70°C, the scattering coefficient nearly doubled, which corresponded to a blanching of the tissue samples. This was followed by a slight decrease for temperatures beyond 70°C. At this wavelength, μ_s was always greater in frozen than in fresh samples. Fresh samples measured at the 633-nm wavelength also showed an increase in μ_s for temperatures up to 65°C (4.88 ± 0.23 to 5.69 ± 0.30 mm^{-1}) followed by a steep increase between 65°C and 75°C to 7.66 ± 0.24. The scattering coefficient for the frozen samples remained constant (5.01 vs. 5.09 mm^{-1}) up to 55°C, after which it increased with temperature to 75°C (11.04 ± 0.56 mm^{-1}) and then fell off slightly with exposure temperatures above 75°C. Although there was no difference in μ_s up to 55°C, the measurements of μ_s in frozen samples were considerably higher than those measured in fresh samples for temperatures above 55°C.

Results from the ANOVA indicated a significant difference in μ_s between wavelengths ($P < 0.05$). Post hoc independent samples, two-tailed t tests, performed with the 35°C and 70°C measurements showed significant differences ($P < 0.05$) between the fresh samples at each wavelength.

Computed values of the anisotropy are presented in Figure 5. For the measurements on the fresh samples, g decreased slightly with exposure temperature up to 65°C and then increased very

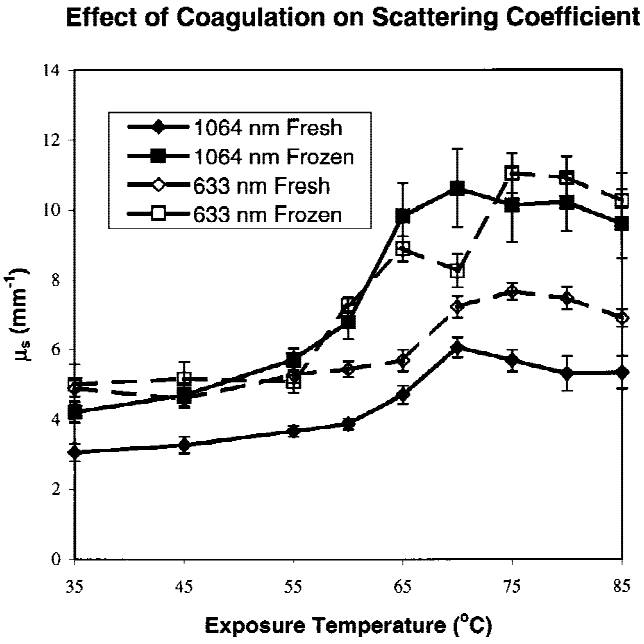

Fig. 4. Scattering coefficients for fresh and previously frozen canine prostate tissue measured at wavelengths of 1,064 and 633 nm (data points represent the mean ± SEM).

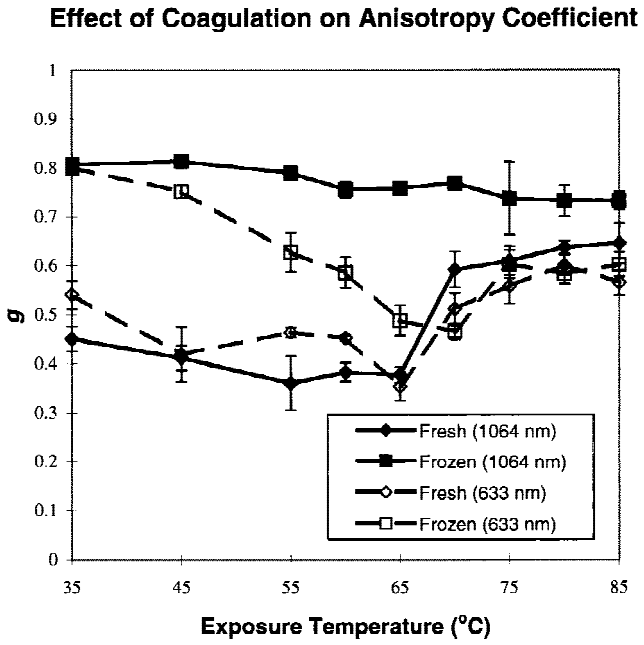

Fig. 5. Anisotropy coefficients measured at 1,064 and 633 nm (data points represent the mean ± SEM).

rapidly. This trend was seen for both wavelengths, and the values between the 1,064-nm and 633-nm measurements appeared similar (0.45 ± 0.03 to 0.38 ± 0.02 for Nd:YAG vs. 0.54 ± 0.02 to 0.35 ± 0.03 for HeNe). For frozen samples measured at 1,064 nm, g remained relatively unchanged during tissue coagulation (0.81 ± 0.01 to 0.73 ± 0.02), whereas the frozen samples measured at 633 nm demonstrated a large decrease in g (0.80 ± 0.01 to 0.47 ± 0.02 before increasing again to ~0.6).

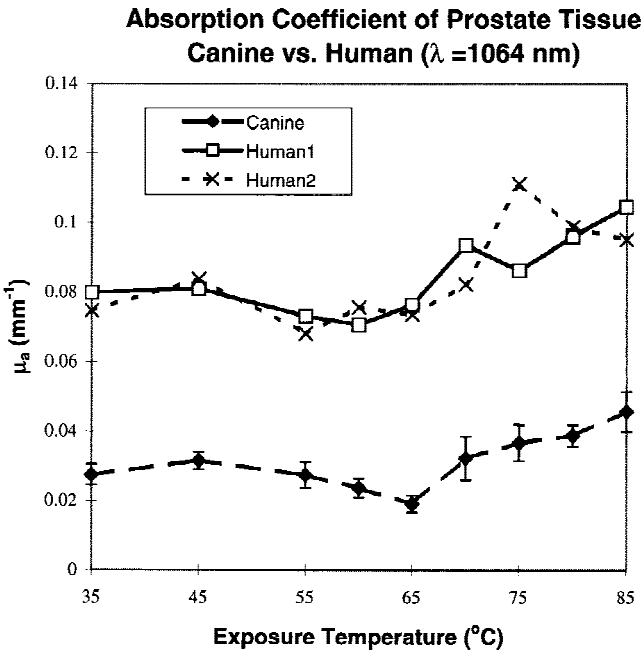

Fig. 6. Comparison of absorption coefficient between fresh human and fresh canine prostate tissue at 1,064 nm.

Although only two fresh human prostates were available, the optical properties of these two samples were very similar. It appears that μ_a and g for human tissue are considerably higher than those for canine tissue (see Figs. 6, 7). The scattering coefficient of human prostate tissue (1.66 ± 0.05 mm^{-1}), however, was approximately one-half that of canine prostate tissue (3.06 ± 0.26 mm^{-1}; Fig. 8).

Results of the analysis of the IAD algorithm showed that the percent difference between the recalculation of the values of the optical properties and the baseline values are linearly proportional to changes in the IAD algorithm input parameters V_r%, V_t%, V_c%, n_t, and d. The percent differences between the recalculated values and the baseline values per a 1% change in the measured input parameters are presented in Table 2. Figure 9 shows the nonlinear relationship between the calculation of μ_s and the default input value chosen for g when V_c% is zero.

DISCUSSION

The optical properties of canine prostate tissue were measured through a range of tempera-

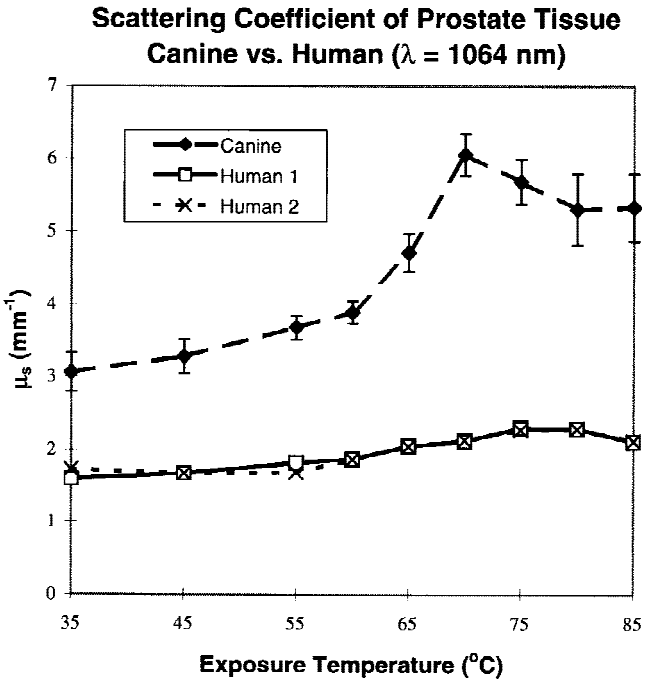

Fig. 7. Comparison of scattering coefficient between fresh human and fresh canine prostate tissue at 1,064 nm.

tures by using the double-integrating sphere method [13]. The values for the absorption and scattering coefficients measured in the present study were consistent with those determined for other soft tissues. The effects of thermal coagulation on optical properties were investigated by exposing tissue samples to temperatures ranging from 35°C to 85°C. Temperature-dependent changes in tissue optical properties are especially important when modeling interstitial or free beam laser thermotherapy. Laser wavelength, intensity, treatment duration, and number of treatment punctures may be determined by the rate of change of the optical scattering and absorption coefficients.

Results from the present study showed that the scattering coefficient nearly doubled as tissue coagulated, whereas the absorption coefficient decreased slightly with increasing exposure temperature to the point of coagulation. The anisotropy coefficients were also seen to decrease with increasing exposure temperature. These trends were also consistent with those of other studies. Effects of storing tissue in a frozen state prior to measuring optical properties were also studied. Freezing tissue caused the absorption, scattering, and anisotropy coefficients to increase for Nd:YAG laser light. This increase is attributed to water begin trapped in the cells at the time of

TABLE 2. Sensitivity of IAD Algorithm to Measured Input Parameters

1% Increase in measured parameter	Percent difference in calculated values			
	μ_a	μ_s	g	μ_s'
V_r%	−4.7	0.03	−1.4	1.26
V_t%	−4.2	0.03	1.3	−1.12
V_c%	−0.22	−0.22	−0.23	−0.02
d	−0.99	−0.99	0	−0.99
n_t	−1.6	0.03	−0.4	0.38

freezing, which expands and ruptures cell membranes or other cellular structures. This would have the effect of creating more scatterers and absorbers of approximately the same size as this wavelength. Freezing had little effect on the properties measured with the HeNe laser, which has a shorter wavelength.

Two anecdotal studies on human tissue were also performed in the present study. Measurements on the human prostate tissue indicated significant differences in the absorption and scattering coefficients than in those measured in fresh canine tissue. This demonstrates the need to exercise caution when attempting to extrapolate data obtained from animal experiments to humans and the need for reliable human data.

Although the absorption coefficients measured in the present study remained relatively unchanged by coagulation, there was a slight decrease as tissue coagulated, followed by a slight increase during exposure to higher temperatures (T > 65°C). It has been suggested that the absorption of photons by chromophores may produce decomposition states that have a decreased absorption [18]. This notion may explain the decrease in measured absorption as the tissue coagulated. The increase in absorption following coagulation was most likely associated with the darkening (browning) of the tissue.

A recent report has suggested that there are two time-dependent processes responsible for changes in the reduced scattering coefficient [19]. The first is characterized by a fast temperature-dependent rate, and the second by a much slower, "erratic" temperature-independent rate. This slower process was attributed to slow shrinkage of the tissue by extrusion of water during heating. Thus, for the measurements collected at temperatures above 70°C, the apparent changes in optical properties may be due to factors other than tissue coagulation. Such factors may include errors due to mismatched boundary conditions at the glass–tissue interface when water has been desiccated

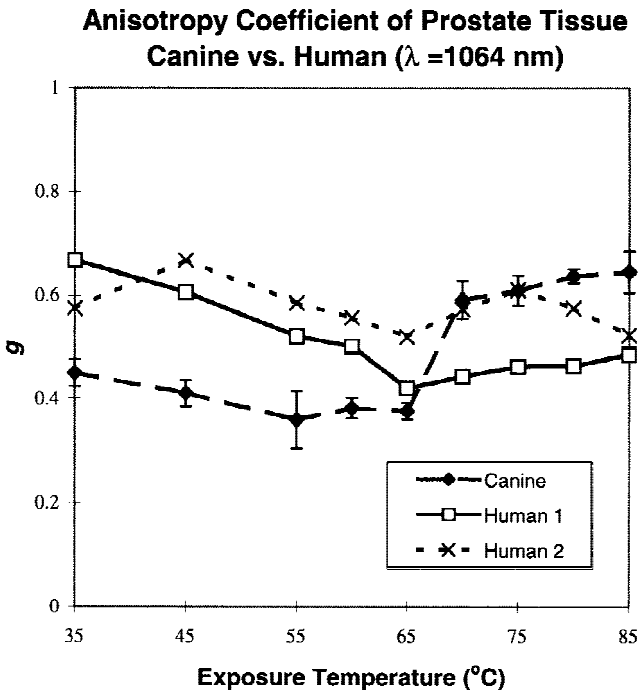

Fig. 8. Comparison of anisotropy coefficient between fresh human and fresh canine prostate tissue at 1,064 nm.

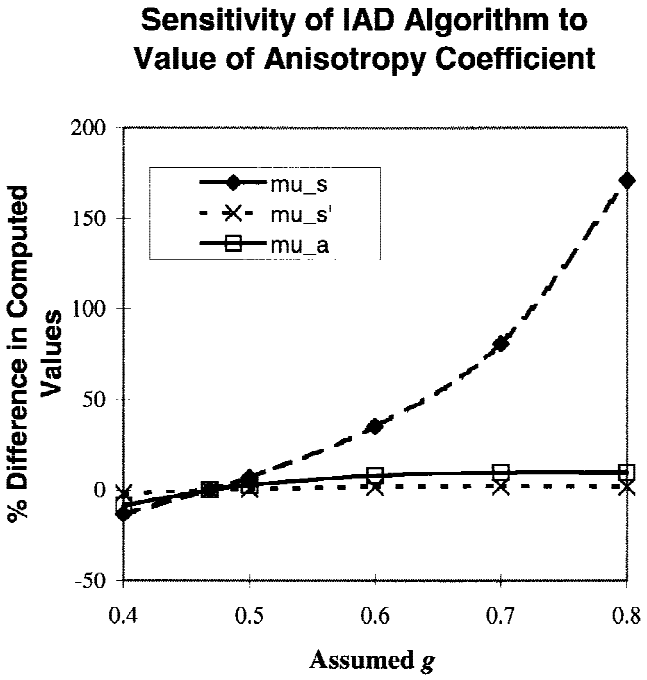

Fig. 9. Sensitivity of IAD algorithm to assumed value of g in the computation of the absorption, scattering, and reduced scattering coefficients.

from the tissue. The sensitivity of the IAD algorithm to the index of refraction of the tissue was seen to have the greatest effect on the computation of the absorption coefficient. If in fact the index of refraction does change with coagulation, measurements of n will prove useful in obtaining accurate measurements of optical properties.

The values of g determined in this study were considerably less than expected. Tissue is generally considered to be highly forward scattering ($g > 0.8$). Although values measured with the HeNe laser were close to 0.8, those obtained for fresh tissue with the Nd:YAG laser ranged from 0.4 to 0.6. Although the analysis of the IAD algorithm showed that computed values of g are most sensitive to the measurements of $V_r\%$ and $V_t\%$ (Table 2), the determination of the anisotropy coefficient requires all three voltage measurements ($V_r\%$, $V_t\%$, and $V_c\%$). Light was detected by the collimated transmittance detector for only three measurements in each of the four groups studied. Thus, it was only possible to determine the values of g for those 12 samples, and no statistical analysis conducted. The measurement of $V_c\%$ is hindered by the total attenuation coefficient ($\mu_t = \mu_a + \mu_s$) of the sample and by the measurement of noncollimated light, which is scattered into the direction of the detector [16]. These factors may have contributed to the low values of g computed at 1,064 nm, and future work will focus on collecting on-axis and goniometric transmission measurements to determine g.

Additional experimental considerations that need to be addressed primarily include the sample dimensions. For frozen samples, obtaining thin slices can be accomplished with relative ease. However, slicing fresh tissue proves to be more difficult, particularly if one wants thin, uniform slices. For thicker slices, light will be lost from the sides of the tissue sample during measurement unless the distance from the edge of the irradiating beam on the sample to the edge of the port (h) is much larger than the lateral propagation of light in the tissue.

$$h >> \frac{1}{\mu_a + \mu'_s}. \quad (2)$$

The IAD algorithm will attribute this loss of light to absorption, resulting in an overestimation of the absorption coefficient [20]. During coagulation, the cross-sectional area of the sample decreases due to loss of water. Because the sample must cover the entire sample port in the sphere, small sample ports (12.7 mm in diameter) were used. In the present study, h was approximately 5.4 mm, and the right side of the inequality

ranged from 0.4 mm to as high as 1.6 mm. Thus, absorption coefficients may be slightly overestimated.

The second consideration concerns the presence of blood in the sample. Because all of the samples came from animals that had been exsanguinated with simultaneous infusion of saline, there may have been little effect on the measurements due to the presence of hemoglobin and other blood constituents.

Another consideration concerns the measurement of sphere coefficients to correct for cross talk of light between the spheres, where light from the transmittance sphere is transmitted back through the sample into the reflectance sphere, and vice versa. The IAD algorithm was designed to compute optical properties whether or not sphere coefficients are entered. Cross talk between the spheres is primarily a problem for very thin samples. Because the sample thicknesses used in the present study were considered fairly thick, the errors induced by cross talk were assumed to be negligible, and the optical properties were calculated without the sphere corrections (Prahl, personal communication). With these considerations in mind, regardless of whether the data represent absolute measures for the optical properties, the differences between fresh and frozen tissue and with coagulation remain valid.

The final consideration concerns the sensitivity of the IAD algorithm to the measured input parameters (V_r%, V_t%, V_c%, d, and assumed g). These parameters were independently changed from baseline values measured with the 1,064-nm laser by ±1%, ±5%, ±10% and ±20%. The optical properties were then recomputed with these new parameters, and percent differences between the new values and the baseline values of the optical properties were calculated. The percent difference between the recalculated values of the optical properties and the baseline values were shown to be linearly proportional to changes in the IAD algorithm input parameters V_r%, V_t%, V_c%, n_t, and d. The analysis indicated that the computation of the absorption coefficient is sensitive to the measurements of reflectance and to transmittance voltages. The scattering coefficient remains relatively unaffected by errors in the measured voltages but is very sensitive to the default value of g used in the program when no value for V_c% is input. As seen in Figure 9, the percent difference between the recalculated values of μ_s and the baseline value (4.17 mm^{-1} at $g = 0.47$) increased exponentially with increasing values for g. This resulted in a 170% difference in the calculation of μ_s when a value $g = 0.8$ was assumed and V_c% was set to 0.00. This further highlights the importance of obtaining accurate measurements for the anisotropy coefficient. The reduced scattering coefficient, however, was relatively insensitive to errors in the input parameters or to the assumed value of g. The anisotropy coefficient was found to be directly proportional to errors in either the reflectance or transmittance measurements. As expected, both μ_a and μ_s are inversely proportional to the measured sample thickness. Neither the scattering coefficient nor the anisotropy coefficient was sensitive to the index of refraction of tissue.

In summary, the optical properties (μ_a, μ_s, μ_s', and g) of fresh and previously frozen canine prostate tissue were measured at two wavelengths over a 50°C temperature range. In the present study, a dependence in optical properties on exposure to elevated temperatures was demonstrated. How the properties changed with temperature was shown to be dependent on both the wavelength used to make the measurements and on the freshness of the tissue. An understanding of the factors affecting optical properties in tissue is fundamental when selecting a wavelength for a specific medical application and when evaluating experimentally obtained values of optical properties. These results will prove useful in the development of models for determining laser dosimetry in clinical applications and for the development and evaluation of new laser delivery devices.

ACKNOWLEDGMENTS

We thank Dr. Scott Prahl for providing the IAD program used in this study and for his advice with experimental considerations. We thank the Department of Urology for providing use of the lasers. Lastly, we offer our appreciation to Dr. George Reed and Dr. Linda Auther for their advice on the statistical analysis of the data.

REFERENCES

1. Modest M. Radiative properties of particulate media. In: Holman JP, Lloyd JR, eds. "Radiative Heat Transfer." New York: McGraw-Hill, Inc., 1993, pp 383–437.
2. Thomsen S. Medical lasers: how they work and how they affect tissue. Cancer Bull 1989; 41:203–210.
3. Patterson M, Chance B, Wilson B. Time resolved reflectance and transmittance for the non-invasive measurement of tissue optical properties. Appl Optics 1989; 28: 2331–2336.
4. Wilson B, Jacques S. Optical reflectance and transmit-

tance of tissues: principles and applications. IEEE J Quant Electr 1990; 26:2186–2198.
5. Splinter R, Svenson R, Littmann L, Tuntelder J, Chuang C, Tatsis G, Thompson M. Optical properties of normal, diseased, and laser photocoagulated myocardium at the Nd:YAG wavelength. Lasers Surg Med 1991; 11:117–124.
6. Cheong W, Prahl S, Welch A. A review of the optical properties of biological tissues. IEEE J Quant Electr 1990; 26:2166–2185.
7. Arnfield M, Tulip J, McPhee M. Optical propagation in tissue with anisotropic scattering. IEEE Trans Biomed Engin 1988; 35:372–381.
8. Chambettaz F, Weible M, Salathe R. Temperature dependence of reflectance and transmittance of the artery exposed to air during laser irradiation. IEEE Trans Biomed Engin 1993; 40:105–107.
9. Derbyshire G, Bogen D, Unger M. Thermally induced optical property changes in myocardium at 1.06 μm. Lasers Surg Med 1990; 10:28–34.
10. Pickering J, Posthumus P, van Gemert M. Continuous measurement of the heat-induced changes in the optical properties (at 1064 nm) of rat liver. Lasers Surg Med 1994; 15:200–205.
11. Çilesiz I, Welch A. Optical properties of human aorta: are they affected by cryopreservation? Lasers Surg Med 1994; 14:396–402.
12. Splinter R, Cheong W, van Gemert M, Welch A. In vitro optical properties of human and canine brain and urinary bladder tissues at 633 nm. Lasers Surg Med 1989; 9:37–41.
13. Pickering J, Prahl S, van Wieringen N, Beek J, Sterenborg H, van Gemert M. Double-integrating-sphere system for measuring the optical properties of tissue. Appl Optics 1993; 32:399–410.
14. Prahl S, van Gemert M, Welch A. Determining the optical properties of turbid media by using the adding-doubling method. Appl Optics 1993; 32:559–568.
15. Troy T. "The Measurement of Tissue Optical Properties Using the Double-integrating Sphere Technique." Master's Thesis. Nashville: Vanderbilt University, 1994.
16. Prahl S. "Optical Property Measurements (IAD Program Users Manual)." September 1994. Available directly from the authors, or from the ftp site laser.mda.uth.tmc.edu/pub/ansic/add-dbl.
17. Glantz S. Experiments when each subject receives more than one treatment. In: Jeffers JD, Englis MR, eds. "Primer of Biostatistics," Ed. 3. New York: McGraw-Hill, Inc., 1992, pp 278–319.
18. Jacques S. Role of tissue optics and pulse duration on tissue effects during high-power laser irradiation. Appl Optics 1993; 32:2447–2454.
19. Agah R, Gandjbakhche A, Motamedi M, Nossal R, Bonner R. Dynamics of temperature dependent optical properties of tissue: dependence on thermally induced alteration. IEEE Trans Biomed Engin 1996; 43:839–846.
20. Torres J, Welch A, Çilesiz I, Motamedi M. Tissue optical property measurements: overestimation of absorption coefficient with spectrophotometric techniques. Lasers Surg Med 1994; 14:249–257.